

THE INFLUENCE OF PREFERENTIAL FRACTURE POINTS ON THE PENETRATION BEHAVIOUR OF KE PENETRATORS AGAINST ANGLED PLATES

N J Lynch¹, R G Townsley¹, A W Bruce¹, P D Church¹ T D Andrews²

¹ *QinetiQ, Fort Halstead, Sevenoaks, Kent TN14 7BP, UK*

² *QinetiQ, Cody Technology Park, Farnborough, Hants, GU14 0LX, UK*

This paper examines the use of a preferential fracture point to improve the perforation behaviour of a KE projectile against an oblique plate. Small scale L/D 25 tungsten alloy projectiles were impacted by an RHA plate using the reverse ballistic technique. The projectiles had a small pitch angle to emphasise the fracture behaviour. A notch was placed at various positions at the front of the projectile length to examine its effect on fracture. A notch placed behind the first sabot interface groove did not change the behaviour, but placing the notch ahead of the first groove caused fracture at the notch rather than the groove. Lagrangian simulations were undertaken with the Goldthorpe path dependent fracture criterion to investigate the effect of notch placement on rod break-up. Lagrangian simulations were able to reproduce the fracture of the projectiles into the same number of segments obtained in the experiments. Fracture at the notch and first groove position were more difficult to reproduce.

INTRODUCTION

During the perforation of oblique target plates, the asymmetry of the process causes lateral flow of projectile material. Depending on the ductility of the projectile material, the extent of the asymmetry, and surface features on the projectile, an amount of the material will separate from the penetrator. This material does not then contribute to subsequent penetration. However, preventing fracture and separation from occurring may be equally deleterious to projectile performance because the lateral momentum of the attached material will cause additional projectile material to bend away from the line of flight.

This paper examines the extent to which features in the projectile can be used to preferentially fracture the penetrator. Creation of favourable fracture points requires control of the surface of the rod to reduce the probability of fracture at undesirable positions and the introduction of features to encourage fracture at the desired location

and time. Lagrangian simulations of some of the experiments were carried out to investigate differences between threaded and unthreaded rods, sensitivity to notch position and sensitivity to fracture parameters. The simulations were performed using the QinetiQ modified Lagrangian hydrocode DYNA3D.

EXPERIMENTS

Targets

The experiments were carried out using the reverse ballistic technique where the target is fired at a stationary projectile. The target was contained in an aluminium launch package and fired from a 40 mm calibre smooth bore gun. The target plate was 5 mm thick and made from Rolled Homogeneous Armour (RHA) steel to UK specification 95/13-1. The hardness of the plates was 346 HV30 (approximately 328 Brinell). The target obliquity was 55.7° from the vertical.

1	2	3	4	5	6	7	8	9	10
CLASSIFIED	Projectiles	PROJECTION	ENGINEERING DRAWING PRACTICE TO BS 8888 UNLESS OTHERWISE STATED:- (1) ALL BURRS & SHARP EDGES TO BE REMOVED. (2) A RADIUS OR CHAMFER OF 0.2 (MAX) IS PERMITTED IN THE CORNERS OF BLIND HOLES, RECESSES & STEPS. (3) REFERENCES TO STANDARDS & SPECS. IMPLY LATEST ISSUE.						COPYRIGHT QinetiQ Ltd. 2006

The tungsten heavy alloy (WHA) projectiles were 78 mm long and had a major diameter of 3.1mm. Grooves were machined into the projectile, starting 16 mm from the impact face to represent the sabot interface thread used on APFSDS projectiles. The thread details are shown in Figure 1. This baseline design was modified in some of the tests to examine the effect of adding fracture notches. Two types of 92% tungsten-nickel-iron alloy were used, as supplied by Cime Bocuze, France. Alloy A had a 0.2% proof strength of 990 MPa, and elongation at failure of 23% and an un-notched Charpy value of 35 J (5 mm specimen). Alloy B had a 0.2% proof strength of 1850 MPa, and elongation of 1 to 5% and an un-notched Charpy value of 5 to 9 J. The projectiles were mounted at a pitch angle to accentuate the fracturing of the tungsten alloys.

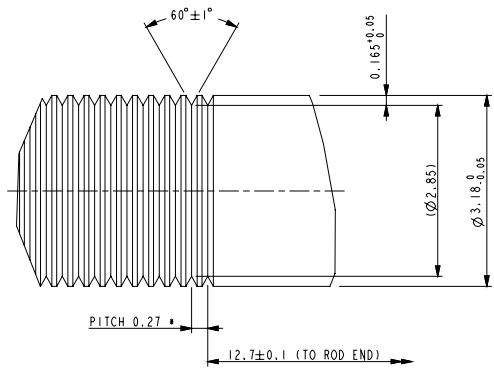


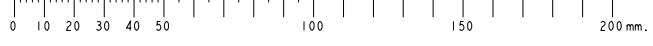
Figure 1 Groove details on the projectile

DETAIL A
SCALE 20:1

WORKING INSTRUCTIONS
COMPONENT TO BE PLACED IN AN APPROVED CONTAINER.
CONTAINER TO BE PERMANENTLY AND LEGIBLY MARKED
WITH DRAWING NUMBER AND LATEST ISSUE.

CHANGE SHEET NUMBER	ISS	DATE
CERTIFICATION NUMBER	DC/06/027	A 26-5-06

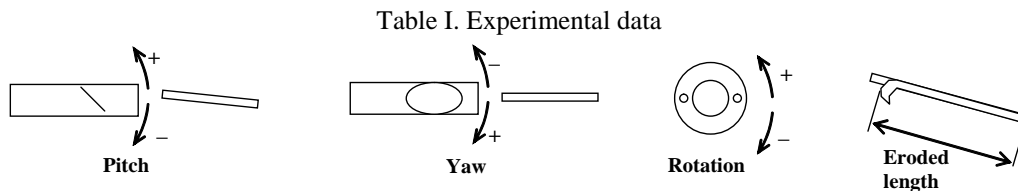
MATERIAL TUNGSTEN (AS SUPPLIED)	FINISH NONE	DIMENSIONS IN mm TOLERANCES - LINEAR ± ANGULAR ± AS STATED	Ltd. FORT HALSTEAD TITLE ROD, BASELINE	SECURITY CLASSIFICATION UNCLASSIFIED
EST. MASS 10.5g @ 17.6g/cc	SURFACE ROUGHNESS 1.6	SCALE 5:1 & 20:1 UNLESS OTHERWISE STATED		QinetiQ DRAWING NUMBER FHD-3040



Results

The results from the eight tests are given in Table 1. The projectile has a natural tendency to rotate in the gun when fired. For tests 5159-5163 the target was loaded into the gun with 25° of pre-rotation, which reduced the rotation at impact to acceptable levels. The primary effect of plate rotation when impacting a pitched attitude projectile is to change the projectile deflection from the vertical to the horizontal plane, but a rotation of up to 10° will have negligible effect (<1%) on the experimental results [1,2]. The highest rotation of 24° (test 5155) will reduce the vertical deflection by 5% compared to an impact without rotation.

The notable difference in the results is the difference in the fracture behaviour between alloy A and B, as shown in Figure 2. Alloy A fractured into three pieces, whereas alloy B fractured repeatedly into four pieces. The increase in fracture was to be expected given the reduced Charpy values of this material. The fracture positions in alloy A were where the first and last groove was located. Alloy B fractured also in the centre. The eroded length stated in Table I is the addition of the centre-line lengths of the fragments. No noticeable difference in the eroded length of the two alloys was observed.



Test No.	Target Velocity (m/s)	Pitch (°) ± 0.25°	Yaw (°) ± 0.25°	Rotation (°) ± 2°	Projectile alloy	Projectile pitch angle (°)	Eroded length (mm) ± 0.5 mm
5153	1572	-0.50	-0.50	+15	B	2.8	67.9
5154	1540	-1.30	-0.75	+22	A	2.3	69.3
5155	1546	-0.25	-0.50	+24	B	2.6	68.4
5159	1566	0	-0.25	+2	A	3.6	68.5
5160	1567	-1.80	+1.00	-11	A	2.5	71.0
5161	1577	-1.30	-0.15	+5	A	2.8	68.0
5162	1557	-1.00	+0.25	0	A	2.4	68.0
5163	1582	+0.50	+0.25	-6.5	B	3.1	68.0

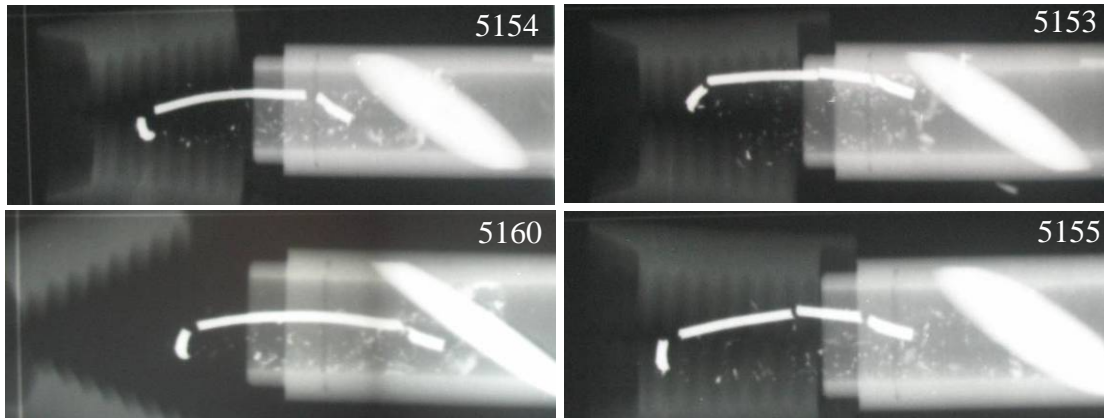


Figure 2. Results from experiments with un-notched projectiles.
LH column Alloy A; RH column Alloy B.

Modifications to the projectile were then made to see whether a fracture notch could be used to either reduce the projectile bending, or to retain more of the projectile by fracturing it ahead of the first groove position. Table II gives the details of the notch depth and position in the four tests. The radiographs from the tests are shown in Figure 3.

Table II. Depth and position of fracture points

Firing No.	Notch depth (mm)	Notch position from front of projectile (mm)
5159	0.33	16.24
5161	0.33	19.42
5162	0.50	19.42
5163	0.33	13.06

For test 5159 the depth of the first groove was increased, doubling the depth from 0.165 mm to 0.33 mm. The radiograph in Figure 3 shows no significant difference in the projectile shape from the un-notched firings. For test 5161 the notch was moved one rod diameter towards the rear of the projectile, and for test 5162 the same position was used, but the depth was increased. The projectile fracture point did not change in either test, though the central portion of the projectile in 5162 is straighter.

For the final test (5163), using alloy B, the notch position was moved ahead of the first groove. This resulted in fracture at the notch position rather than the first groove. No further projectiles in alloy A were available to confirm whether this alloy would also fracture with a notch in this position.

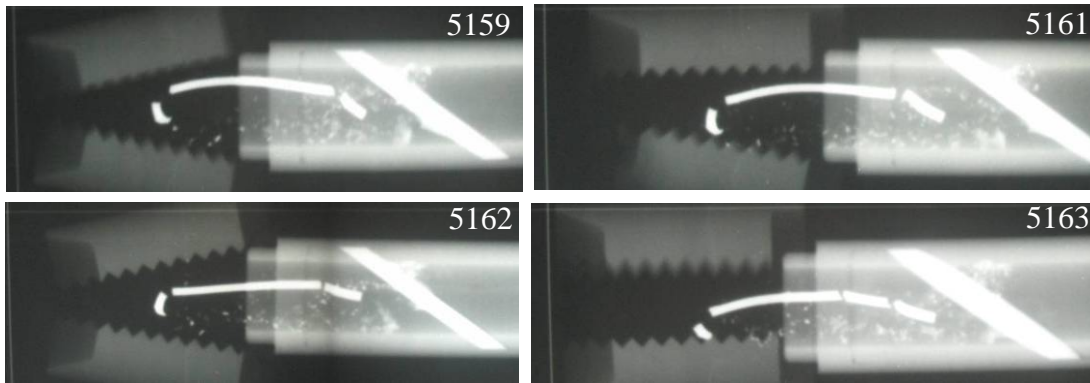


Figure 3. Results from experiments with notched projectiles.

SIMULATIONS

Constitutive & Fracture Models

The treatment of fracture within a hydrocode is not simply the definition of a fracture criterion. The prediction of fracture is dependent on the constitutive model applied, which determines the stress distribution, as well as the applied fracture criteria. Modified Armstrong-Zerilli BCC constitutive models [3,4] have been used to represent the steel target plate and the WHA projectile. The fracture model used in the projectile and the target was the Goldthorpe Path Dependent Fracture (PDF) model [5], which is based on ductile void growth within an isotropic material under different stress states. The damage increment is given as:

$$dS = 0.67 \int_0^{\varepsilon} \exp[1.5 \sigma_n - 0.04 \sigma_n^{-1.5}] d\varepsilon + A \varepsilon_s \quad (1)$$

where dS = damage increment, σ_n = Pressure/Yield (POY), ε = effective plastic strain, ε_s = shear failure strain and A = constant determined for torsion test. The damage is then incremented by:

$$S_{new} = S_{old} + dS \quad (2)$$

Fracture occurs when the damage reaches a critical value S_c (also known as the void fracture number vfn), which is determined from a quasi-static tension test. The damage comprises a tensile component due to void growth and a shear component due to shear localisation. The shear parameter 'A' (or shm) is determined from a torsion test, which measures the shear strain to failure. Thus the algorithm is a multi-mode failure model, where the tensile failure will dominate for P/Y values less than -0.3 and the shear failure will dominate for the P/Y values between -0.3 and zero.

A complication with WHA's is that they exhibit a complex intergranular-transgranular failure mechanism which is a strong function of strain rate and temperature. The Goldthorpe PDF model is an approximation and has essentially been fitted to the experimental notched tensile tests to provide a value for v_{fn} and sh_m . In this study it was not possible to test alloy A and B and so the fracture parameters were estimated from previous work on another WHA.

Effect of Notch Position

Three DYNA3D simulations were undertaken based on the geometry of test 5162. Each simulation considered that the projectile was constructed from alloy A, and the sabot grooves were represented as an average diameter, such that the threads were not explicitly simulated. The first simulation utilised the projectile design from test 5153 (i.e. with no notch). The second was a simulation of test 5162, where the notch was placed one rod diameter into the grooved region, while the third was based on 5163 with a notch one diameter forward from the first groove. All projectiles had a pitch of 2.8° and a plate velocity of 1557 m/s. The rear notch depth was 0.5 mm while the forward notch depth was 0.33 mm as in the experiments. The results for the rod break-up are shown in Figure 4.

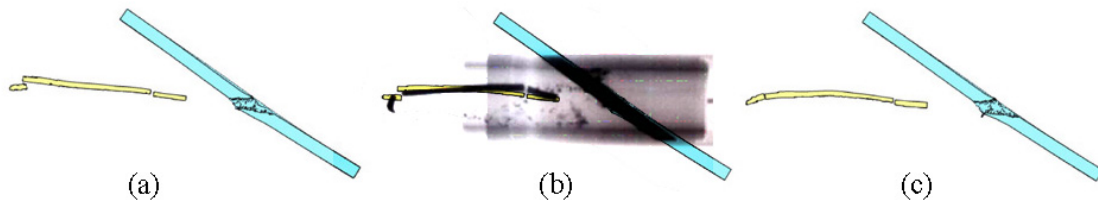


Figure 4. Alloy A projectiles with no notch (a), rear notch (b) and forward notch (c)

Figure 4 (a) and (b) show the fracture occurring at the first groove as in the experiment. Case (c) however did not fracture at the forward notch. This prediction may be correct however, as the analogous experiment has not been undertaken with alloy A. To determine whether the averaged diameter was affecting the fracture behaviour, simulations were then run with the grooves included.

Effect of Grooves or Threads in Rod

These simulations used DYNA3D to model experiment 5153 using fracture parameters for alloy B. The DYNA computational mesh for the threaded projectiles utilised a replication of a single groove to produce the geometry shown in Figure 5. The machined grooves had a blend radius at the root of 0.06-0.09 mm, whereas for simplicity the simulations did not include this radius.

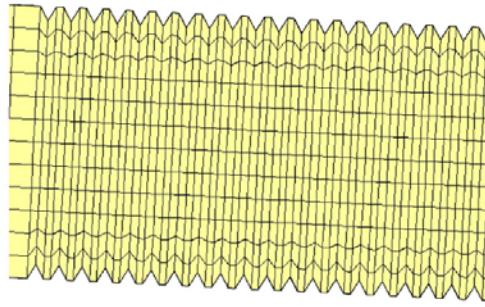


Figure 5. Section through grooved projectile showing computational mesh

The results are shown in Figure 6 for the rod after perforation of the plate compared to the experimental radiograph. The threaded rod simulation reproduces quite accurately the four segment fracture as seen in the alloy B experiments, but the front segment has failed about one rod diameter further back, i.e. not at the first groove position.

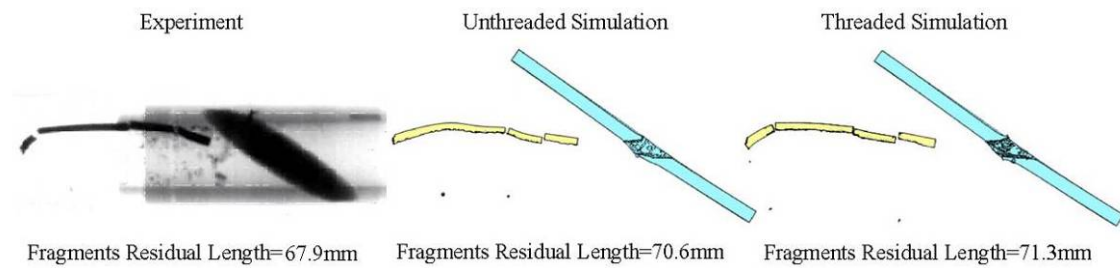


Figure 6. Simulated Alloy B projectiles with and without grooves compared to test 5153

In the last DYNA simulation, the vfn value was reduced by 25% to assess whether this would move the fracture point to the first groove. Figure 7 shows the effect of such a change for two simulations of experiment 5153. The lower fracture value is shown on the left. The effect has been to move the middle fracture position forwards, but the front fracture position is still about one rod diameter behind the first groove.

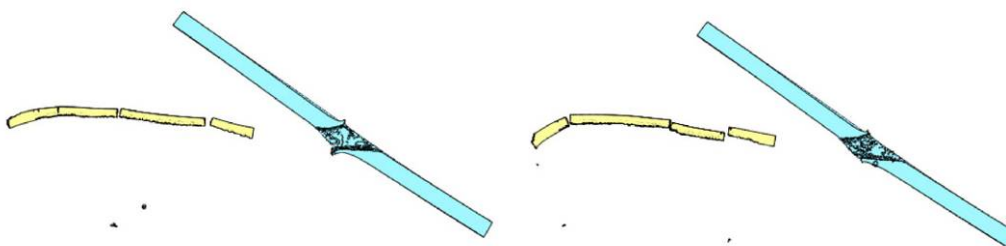


Figure 7. Alloy B rod break-up sensitivity for 25% change in vfn parameter

A possible cause of the difference is that in the experiments the nose rotated more than in the simulations. Deletion of failed elements in the DYNA3D simulations may be reducing the lateral deflection of the projectile nose, which in turn moves the maximum stress position in the projectile rearwards. This work illustrates that whilst the Goldthorpe PDF model is big step forward in simulating the fracture of WHA's, more work is required to fully understand and model the fracture processes in these materials.

CONCLUSIONS

The use of a notch to provide preferential fracture in a KE projectile has been examined. A notch placed behind the first sabot interface groove did not change the fracture behaviour, but placing the notch ahead of the first groove caused fracture at the notch rather than the groove. An additional projectile diameter of material was thus retained, which would contribute to the penetration of subsequent plates in a multiple plate target.

Lagrangian simulations were able to reproduce the fracture of the projectiles into the same number of segments obtained in the experiments. The explicit representation of grooves in the simulations is crucial for the prediction of alloy B fracture behaviour. Fracture at the notch and first groove position was more difficult to reproduce when the sabot interface grooves were included. Further investigation is required in characterising the fracture behaviour of WHA as a function of strain rate and temperature.

REFERENCES

- [1] Liden, E. Andersson, O. and Johansson, B. Influence of the direction of flight of moving plates interacting with long rod projectiles, Proceedings of 20th International Symposium on Ballistics, Orlando, Florida, September 2002.
- [2] Liden, E. Influence of projectile material on yawed long rod projectiles penetrating oblique plates, proceedings of 22nd International Symposium on Ballistics, Vancouver, Canada, November 2005.
- [3] Zerilli, F.J., Armstrong, R.W. Constitutive relations for the plastic deformation of metals, High-Pressure Science and Technology – 1993. American Institute of Physics, Colorado Springs, Colorado, pp. 989-992.
- [4] Butler, A. Church, P. Goldthorpe, B. A Wide ranging Constitutive Model for bcc Steels, , Jnl de Physique C8-471, 1994.
- [5] Goldthorpe, B. D. A path dependent model for ductile fracture, J. Phys. IV France Colloq. C3 (EURODYMAT 97) Vol. 7 pp. 705-710.

© QinetiQ 2006

This work was carried out as part of the Weapon and Platform Effectors Domain of the MoD Research Programme. The contribution of John Stubberfield is also acknowledged.